Building a bridge between industry and theory on the example of a new ventilation system

Kazimierz Peszyński[1,*]

[1]UTP University of Science and Technology in Bydgoszcz, Faculty of Mechanical Engineering, Kaliskiego 7, Poland

Abstract. The paper presents the possibilities of simplified determination of the air volumetric flow rate in ventilation ducts. This problem occurred during the tests of local losses in the elements of a new ventilation system based on ducts with a rounded rectangular cross-section. The presented method requires mathematical modelling of the flow velocity distribution in the ducts. The paper presents four models of the velocity distribution. The necessity of using so many models resulted from the wide coverage of the tested sections: $A_{max}/A_{min} = 46.88$.

Motto
An error of 10 percent (or more) in friction factors calculated using the relations in this chapter is the "norm" rather than the "exception."
(Yunus A. Çengel, John M. Cimbala: Fluid Mechanics – Fundamentals and Applications: Chapter 8. Flow in pipes, p. 322)

1 Introduction

An engineering device (e.g. ventilation, heating and air conditioning systems) can be studied either experimentally (testing and taking measurements) or analytically (by analysis or calculations). The experimental approach has the advantage that we deal with the actual physical system, and the desired quantity is determined by measurement, within the limits of experimental error. However, this approach is expensive, time-consuming, and often impractical. Besides, the system we are studying may not even exist. For example, the entire ventilation systems of a building must usually be sized before the building is actually built on the basis of the specifications given. The analytical approach (including the numerical approach) has the advantage that it is fast and inexpensive, but the results obtained are subject to the accuracy of the assumptions, approximations, and idealizations made in the analysis. In engineering studies, often a good compromise is reached by reducing the choices to just a few by analysis, and then verifying the findings experimentally.

2 Ventilation system developed

In ventilation systems, as in air conditioning, the basic cross-sections are rectangular and circular cross-sections. Both types have their own advantages and disadvantages. In this work, ducts with a rounded rectangular cross-section are analysed, this cross-section is to combine the advantages of both above-mentioned shapes of ventilation ducts.

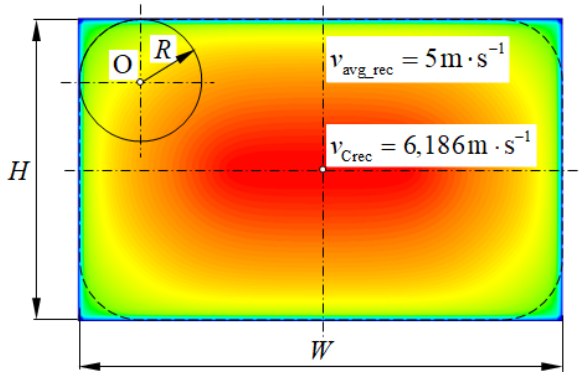

Fig. 1. Velocity distribution of air in rectangular cross-section.

Fig. 1 presents the distribution of air velocity in a rectangular cross-section with dimensions $W \times H = 0.8\,\mathrm{m} \times 0.5\,\mathrm{m}$ obtained during simulation in the ANSYS-FLUENT code, where the average velocity in the duct was entered at the duct input 10 m upstream from the presented analysed duct cross-section.

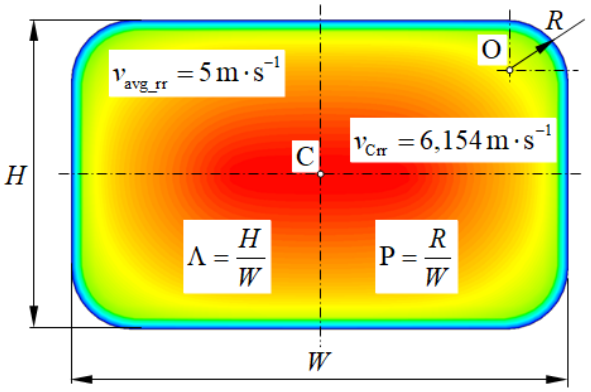

Fig. 2. Velocity distribution of air in rounded rectangular cross-section, Λ , P – nondimensional parameters.

* Corresponding author: peszyn@utp.edu.pl

In Fig. 2 has been defined nondimensional parameters of rounded rectangle cross-section, which are used to generalize derived equations.

Note that $v_{Crr} < v_{Crec}$, this is not a surprising result because it was expected for the same average velocity v_{avg}. This result obtained on by numerical simulation testifies more uniform filling of the cross-section of the rectangle with rounded corners.

2 Models of velocity distribution

The fundamental problem of the experimental studies of system elements properties (mainly local losses) was to determine the flow rate in the ventilation duct $\dot{V}$ ... . From flow rate $\dot{V}$ we can obtain average velocity v_{avg} in examined cross-section. For rounded rectangle is

$$v_{avg\_rr} = \frac{\dot{V}_{rr}}{A_{rr}} \tag{1}$$

where: A_{rr} – rounded rectangular area (see Fig. 2)

$$A_{rr} = W \cdot H - (4-\pi)R^2 = \left(\Lambda - (4-\pi)\mathrm{P}^2\right)W^2 \tag{2}$$

2.1. Basic power-law velocity profile in uniform cross-section

In this model, it is assumed that the velocity distribution over the entire cross-sectional area of the duct is determined by the same formula, known as power-law velocity profile. The adjective "uniform" has been added in the title of this subsection, because in subsections 2.3 and 2.4 the cross-section divided into two parts will be analysed.

At the basis of the analysis of velocity distribution in a rounded rectangular lies the assumption that along the axis of the duct symmetry the velocity distribution is determined by the power-law velocity profile. The maximum velocity is at the central point C, i.e. at the intersection of the rectangle's symmetry axis.

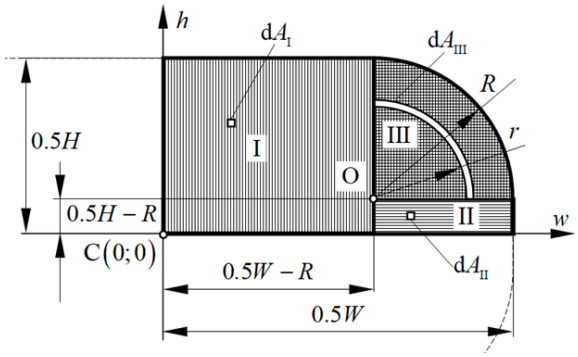

Fig. 3. One quarter of the channel cross-section

That the velocity distribution $v_{rr1}(w,h)$ in the duct cross-section is determined by formula:

$$v_{rr1}(w,h) = v_C\left(\left(1-\frac{w}{0.5W}\right)\left(1-\frac{h}{0.5H}\right)\right)^{\frac{1}{n}} \tag{3}$$

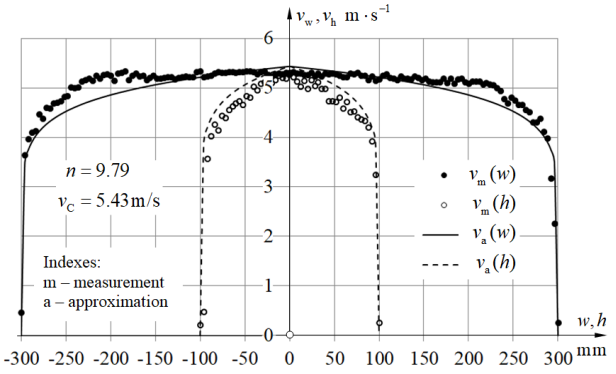

Fig. 4. Approximation of the velocity distribution using the basic power-law velocity profile

Integration formula (3) over this duct quarter area was presented in [1,2]. Average velocity is determined by formula

$$v_{avg1} = \frac{\dot{V}_{rr}}{A_{rr}} = \frac{\frac{n}{n+1}}{\Lambda - (4-\pi)\mathrm{P}^2} \left(\frac{n}{n+1}\Lambda\left(1-\left(\frac{4\mathrm{P}^2}{\Lambda}\right)^{\frac{n+1}{n}}\right)+\pi\left(\frac{4\mathrm{P}^2}{\Lambda}\right)^{\frac{1}{n}}\frac{2n\mathrm{P}^2}{2n+1}\right)v_C \tag{4}$$

2.2. Modified power-law velocity profile in uniform cross-section

Modification of power-law velocity profile consists in putting a squares into it,

$$v_{rr2}(w,h) = v_C\left(\left(1-\left(\frac{w}{0.5W}\right)^2\right)\left(1-\left(\frac{h}{0.5H}\right)^2\right)\right)^{\frac{1}{m}} \tag{5}$$

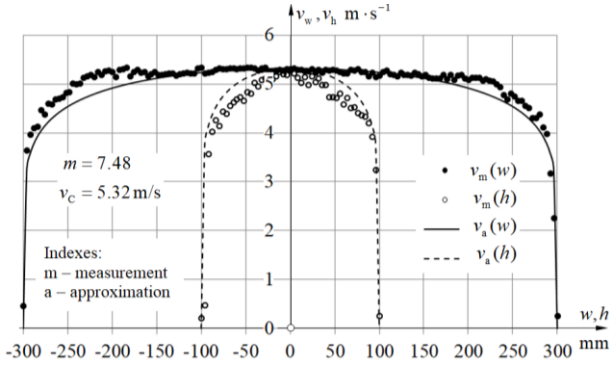

Fig. 5. Approximation of the velocity distribution using the basic power-law velocity profile

The formula (5) obtained as a result of integration of the distribution function over quarter of duct area (Fig. 3) was also presented in [1,2]. In the rounded rectangle, integration problem creates a cross-section area, i.e. the integration surface, however, this area can be divided into three components that have a shape that allows integration. According to Fig. 3, due to symmetry, only a quarter cross-section was integrated. The volume flow rate at approximation using the basic power-law velocity profile was determined as $\dot{V}_{rr1}$, while at the approximation using modified power-law velocity profile (the next

subsection) was marked $\dot{V}_{rr2}$. Flow rate is determined by formula

$$\dot{V}_{rr2} = \left\{ 4\left[\frac{\Gamma\left(1+\frac{1}{m}\right)}{\Gamma\left(\frac{3}{2}+\frac{1}{m}\right)}\right]^2 + \left(\frac{\mathrm{P}^2(1-\mathrm{P})(H-\mathrm{P})}{(0{,}25\mathrm{P})^2}\right)^{\frac{1}{m}} + \mathrm{P}^2\left(\frac{m}{m+1} - \left[\frac{\Gamma\left(1+\frac{1}{m}\right)}{\Gamma\left(\frac{3}{2}+\frac{1}{m}\right)}\right]^2\right)\right\} W^2 v_C \quad (6)$$

2.3. Basic power-law velocity profile in slot-rounded square cross-section

The considerations in subsections 2.1 and 2.2 were tested experimentally. Satisfactory confirmation of the mathematical analysis was obtained for smaller cross-sections of ventilation ducts, $A_{rr} < 0.25\,\mathrm{m}^2$. This mainly concerned rounded rectangular cross-sections for $\Lambda < 0.5$. Therefore, it was necessary to find a new model of flow velocity distribution in the cross-section. During the tests, it was noticed that in the wide coordinate w range around the central point C, the flow local velocity does not change. This suggests the presumption that the velocity distribution in this area is similar to the velocity distribution in the slot. This observation confirms the well-known fact that the Reynolds number calculated on the basis of hydraulic diameter D_h for cross-sections different from circular ones, better reflects the similarity of flows if the cross-section is more similar to circular, e.g. square, hexagon, etc. Therefore, in the new model, it has been assumed that the flow in the channel has a twofold character: one-dimensional as in the slot and two-dimensional as in the circular cross-section (Fig. 6).

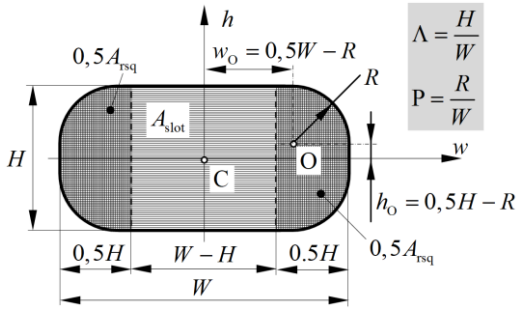

Fig. 6. The division of the cross-section due to the nature of the flow: one-dimensional A_{slot} and two-dimensional A_{rsq}

The cross-section marked in Fig. 6 as A_{slot} is a rectangle with dimensions $w \times h = (W-H)H$. It was assumed that the flow rate in this cross-section is similar to the flow in a horizontal, infinitely wide $w \to \infty$ slot with a height H. This means that the flow velocity in this section depends only on the w variable and is independent of the variable h. Along the axis of the slot, the velocity is maximum and is equal to v_C. The two side parts of the duct cross-section form a virtual rounded square, in Fig. 2.5 it is marked as A_{rsq}. For parameter $R = 0\ (\mathrm{P} = 0)$, this cross-section becomes a square of area $A_{rsq} = H^2$, while for this section it becomes a circle with an area $A_{cir} = A_{rsq} = 0.25\pi H^2 = 0.25\pi \mathrm{P}^2 W^2$.

Based on the above analysis, we can write

$$v_{rsq1} = \begin{cases} \text{for} \quad h \in \langle 0; W-H \rangle & v_C \\ \text{for} \quad w \in \langle 0; H \rangle \\ \quad\ h \in \langle 0; H \rangle & v_C \left(1 - \frac{h}{0.5H}\right)^{\frac{2}{n}} \end{cases} \quad (7)$$

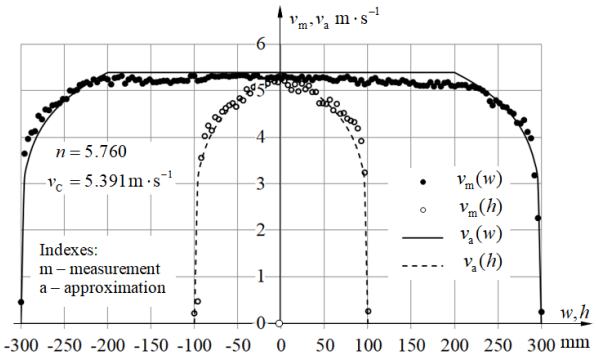

Fig. 7. Approximation of the velocity distribution using the basic power-law velocity profile for slot-rounded square model on the basis of all measurements.

The speed distribution shown in Fig. 7 determined on the basis of all measurements (along the w and h axes) is partly inconsistent with the assumption of the model. The maximum value v_C is determined based on all measurements along the axis w in the range $w \in \langle -0.5(W-H); 0.5(W-H) \rangle$. Fig. 8 shows the velocity distribution solely on the basis of measurements along the shorter axis h of cross-section, because in the assumed model, it was assumed that this axis determines the distribution of the velocity of the flowing air.

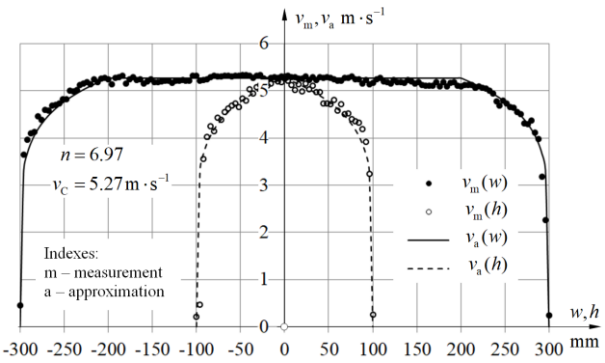

Fig. 8. Approximation of the velocity distribution using the basic power-law velocity profile for slot-rounded square model on the basis of measurements along h axis only.

In this case, the value of v_C is the effect of matching the measured points along the h-axis with the model's curve using the least-squares method.

Integration of formula (7) over area A_{rsq} (Fig. 6) was also presented in [3]. Flow rate is determined by formula

$$\dot{V}_{rr} = \frac{n}{n+1}\left[(1-\Lambda)\mathrm{P} + \left(\frac{n}{n+1}\mathrm{P}^2\left(1-\left(4\mathrm{P}^2\right)^{\frac{n+1}{n}}\right) + \pi\left(4\mathrm{P}^2\right)^{\frac{1}{n}}\frac{2n\mathrm{P}^2}{2n+1}\right)\right]W^2 v_C \quad (8)$$

2.4. Modified power-law velocity profile in slot-rounded square cross-section

Based on experimental research, it can be assumed that for large cross-sections the model resulting from the modified power-law velocity profile is better than the model defined by its original version. According to the modified power-law velocity profile, the flow velocity distribution along the coordinate is given by the formula

$$v_{slot2}(h) = v_C\left(1-\left(\frac{h}{0,5H}\right)^2\right)^{\frac{1}{m}} \quad (9)$$

For this type of model, formula (7) takes the form

$$v_{rsq2} = \begin{cases} \text{for} \quad h \in \langle 0; W-H\rangle & v_C \\ \text{for} \quad w \in \langle 0; H\rangle \\ \quad\; h \in \langle 0; H\rangle & v_C\left(1-\left(\frac{h}{0.5H}\right)^2\right)^{\frac{2}{m}} \end{cases} \quad (10)$$

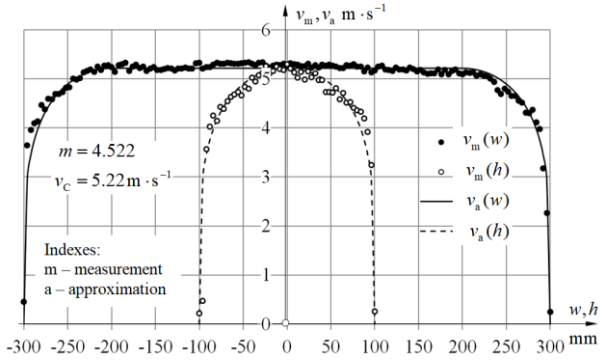

Fig. 9. Approximation of the velocity distribution using the modified power-law velocity profile for slot-rounded square model on the basis of all measurements.

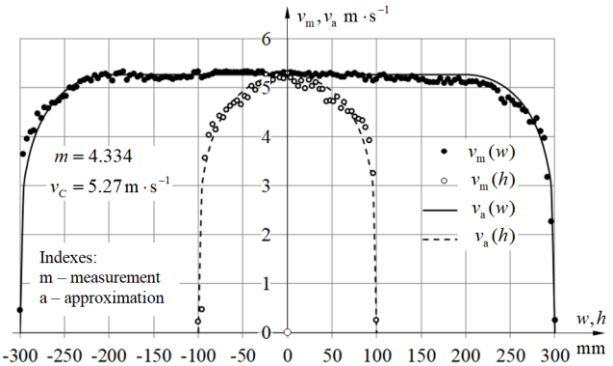

Fig. 10. Approximation of the velocity distribution using the modified power-law velocity profile for slot-rounded square model on the basis of along h axis only.

As in subsection 2.3, the velocity distribution was also determined exclusively on the basis of measurements along the h axis. The result is shown in Fig. 10.

Integration of formula (10) over area A_{rsq} (Fig. 6) was also presented in [3]. Flow rate is determined by formula

$$\dot{V}_{rsq2} = \left[\frac{\Lambda^2}{4}\left[\frac{\Gamma\left(1+\frac{1}{m}\right)}{\Gamma\left(\frac{3}{2}+\frac{1}{m}\right)}\right]^2 + \mathrm{P}^2\left(\frac{4\mathrm{P}(\Lambda-\mathrm{P})}{\Lambda^2}\right)^{\frac{2}{m}}\left(\frac{m}{m+1} - \left[\frac{\Gamma\left(1+\frac{1}{m}\right)}{\Gamma\left(\frac{3}{2}+\frac{1}{m}\right)}\right]^2\right)^{\frac{2}{m}}\right]W^2 v_C \quad (11)$$

3 Measurement only in two points of cross-section area

Approximation was also made based on selected measurement points. The author of this paper is aware of the fact that the measurement along the axis of symmetry of the duct with a small step (4 mm as in the presented example) in industrial conditions is practically impossible. Therefore, the value was determined on the basis of the measured value of the air flow velocity at the appropriate point B located at a distance h_B from the duct wall and lying on the axis of symmetry of the ventilation duct – see Fig. 11, [4, 5].

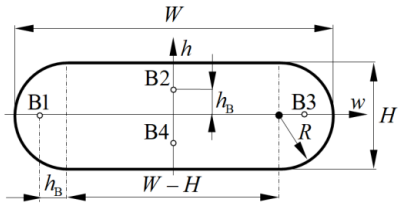

Fig. 11. Cross-section used for comparative studies of the analysed models

The dimensions of this cross-section were: $W = 0.6\,\mathrm{m}$, $H = 0.2\,\mathrm{m}$, and $R = 0.1\,\mathrm{m}$.

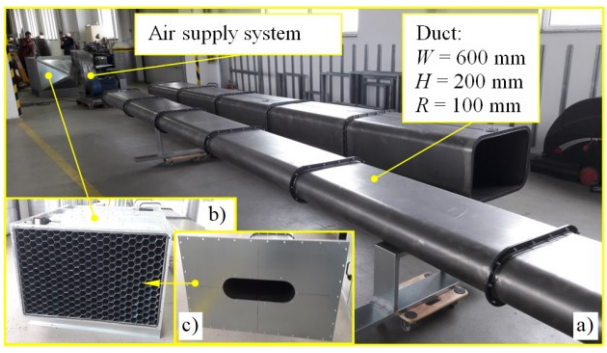

Fig. 12. Preparation of the channel for measurements: a) general view, b) tubular air deflector, c) mask of the tubular air deflector

First, the value was v_C calculated on the basis of four points that were available as a result of measurements $v_B = 0,25(v_{B1} + v_{B2} + v_{B3} + v_{B4}) = 4,755\,\mathrm{m\cdot s^{-1}}$. This value was used to calculate n from the equation which determine the velocity distribution model

$$v_B = v_C\left(1 - \frac{h_B}{0,5H}\right)^{\frac{1}{n}} \tag{12}$$

After lifting both sides of the equation (12) to the power n and substitution $h_B = 0.25H$, it was possible to determine the value n from the equation:

$$n = \frac{\log 0,5}{\log\left(\frac{v_B}{v_C}\right)} \tag{13}$$

After substitution $v_C = 5,27\,\mathrm{m\cdot s^{-1}}$ and $v_B = 4,755\,\mathrm{m\cdot s^{-1}}$ there was obtained $n = 6,76$ – see Fig. 13.

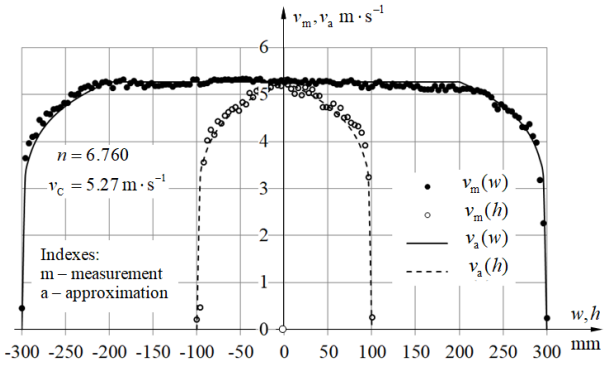

Fig. 13. Model slot – rounded square with using basic power-law velocity and velocities in points B_i and C (Fig. 11).

Similar to the model slot – rounded square with using basic power-law velocity for model slot – rounded square with using modified power-law velocity calculation of m was made. The value of m was determined from the equation

$$v_B = v_C\left(1 - \left(\frac{h_B}{0,5H}\right)^2\right)^{\frac{1}{m}} \tag{14}$$

After lifting both sides of the equation (14) to the power m and substitution $h_B = 0.25H$, it was possible to determine the value m from the equation:

$$m = \frac{\log 0,75}{\log\left(\frac{v_B}{v_C}\right)} \tag{15}$$

In this case, the value v_C is determined solely on the basis of one measurement. This value may be charged with an accidental error. It must be admitted that while calculating the value of m, there was a moment of doubt in the idea of measuring the velocity only at two points B and C. The value of m calculated on the basis of equation (14) is very sensitive to the value of v_C. The $v_B = 4.77\,\mathrm{m\cdot s^{-1}}$ value read for $h = 50\,\mathrm{mm}$ was far from the later obtained theoretical curve of the model, value $m = 2.79$ was obtained. The theory presented above refers to the ideal measurement conditions, first of all, there must be no vibrations of the tested duct. This effect, however, cannot be avoided in industrial research. In order to limit the impact of disturbances, the velocity at points C and B was measured many times, it was assumed that 300 measurements would be sufficient. The effect of this assumption is shown in Fig. 13.

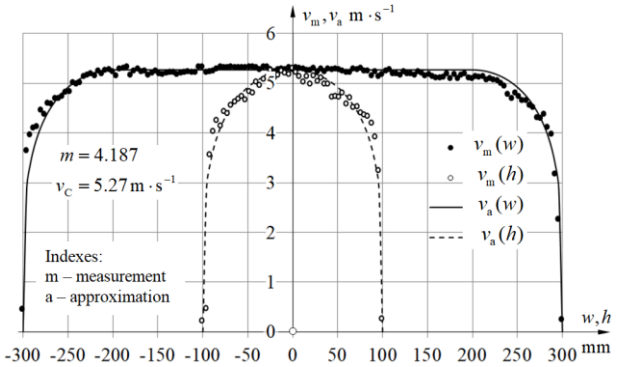

Fig. 14. Model slot – rounded square with using modified power-law velocity and velocities in points B_2 and C (see Fig. 11).

Measurements performed for 5 minutes, and recording the result every one second, allowed to determine the average velocities in time $\bar{v}_C = 5,27\,\mathrm{m\cdot s^{-1}}$ and $\bar{v}_B = 4,92\,\mathrm{m\cdot s^{-1}}$, the result was $m = 4.187$. The configuration of the measurement system is shown in Fig. 14.

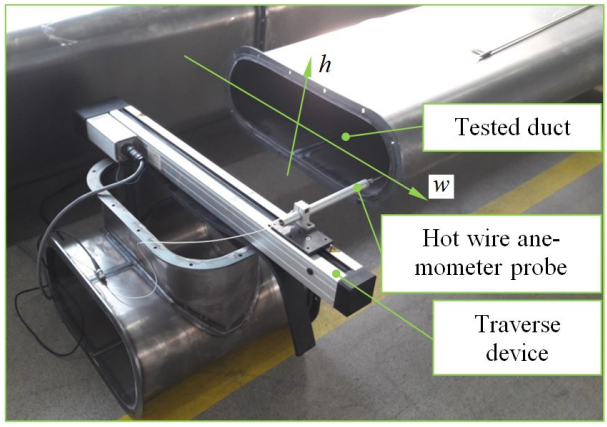

Fig. 15. The principle of measuring the distribution of air velocity in the ventilation duct

5 Conclusions

An analyst working on an engineering problem often finds himself in a position to make a choice between a very accurate but complex model, and a simple but not-so-accurate model. The right choice depends on the situation at hand. The right choice is usually the simplest model that yields satisfactory results. Also, it is important to consider the actual operating conditions

when selecting equipment. There are many significant real-world problems connected with ventilation, heating, and air conditioning systems that can be analysed with a simple model. But it should always be kept in mind that the results obtained from an analysis are at best as accurate as the assumptions made in simplifying the problem. Therefore, the solution obtained should not be applied to situations for which the original assumptions do not hold.

The average air velocity in the ventilation duct plays a significant role. On the one hand, it should not exceed $v_{avg} = 5\text{m}\cdot\text{s}^{-1}$ due to the loudness of the system operation (in industrial power supply ducts can be larger), on the other hand it cannot be too small. During the tests, however, a mistake was made. It was tried, at all costs, to maintain a constant Reynolds number of $\text{Re} = 10^5$ for all cross-sections, changing the flow rate of air. This led to a large dispersion of research results – see Fig.15.

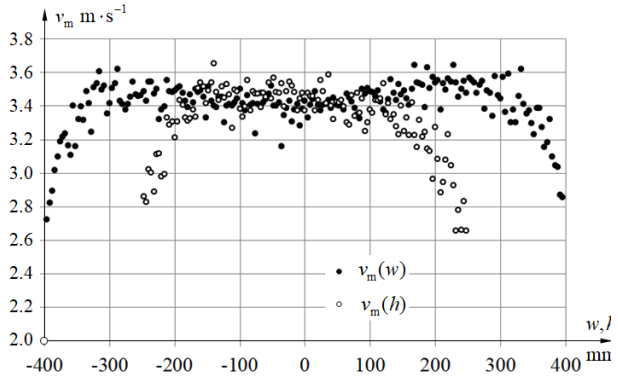

Fig. 16. Distribution of measured velocities for too low average velocity.

Due to the above described behaviour of the air flow, the assumption, which allowed to compare the results was changed. The average air velocity in the channel was taken as the reference value – see Fig.16.

v_{avg} [m·s^{-1}]		*W* [m]										
		0.3	0.4	0.5	0.6	0.8	1.0	1.2	1.4	1.6	1.8	2.0
H [m]	0.2	**6.0**	**5.4**	**5.0**	5.0	5.0						
	0.3	**5.2**	5.0	5.0	5.0	5.0	5.0					
	0.3	5.0	5.0	5.0	5.0	5.0	5.0	5.0				
	0.4	5.0	5.0	5.0	5.0	5.0	5.0	5.0	5.0			
	0.5	5.0	5.0	5.0	5.0	5.0	5.0	5.0	5.0	5.0		
	0.6	5.0	5.0	5.0	5.0	5.0	5.0	5.0	5.0	5.0	5.0	5.0
	0.8	5.0	5.0	5.0	5.0	5.0	5.0	5.0	5.0	5.0	5.0	5.0
	1.0	5.0	5.0	5.0	5.0	5.0	5.0	5.0	5.0	5.0	5.0	5.0
	1.2	5.0	5.0	5.0	5.0	5.0	5.0	5.0	5.0	5.0	5.0	5.0

Fig. 17. Dimensions of developed ventilation system.

Only for the four smallest cross-sections, to preserve values $\text{Re} \geq 10^5$ tests were carried out at slightly higher velocities.

Duct with dimensions $W \times H = 0.6\text{m} \times 0.2\text{m}$ was chosen because it was possible to verify the flow rate calculated on the basis of the formulas, by measuring the flow rate using a volumetric flowmeter "testo". Flowmeter "testo" was mounted on the fan inlet. This solution allows to use this measurement device for many cross-section measurements. Of course, it is assumed that the amount of incoming air is equal to the amount of exhaust air from duct line.

Equations (4), (6), (8), and (11) used to calculate the flow rate look terrible, but modern computing is doing well with them. The flow rates calculated with the aforementioned equations did not differ from the results "testo" flowmeter by more than 7%. Flowmeter "testo" allows to measure the volume flow rate of air in the range $\dot{V}$ -1.2⟩ m^{3}s^{-1}. It has own tubular deflector to calm the input flow.

Author presents four velocity distribution models that may be used for analytical determination of the average velocity in the investigated ventilation ducts. It should be noted that the volume flow rate (or average velocity) is the basic parameter for when designing the ventilation systems. During laboratory tests of the ventilation system components, knowledge of average velocity in ducts is a prerequisite, especially for determining local losses.

Thanks to the development and checking of equations (4), (6), (8), and (11), it was possible to quickly test the properties of the elements (for example arches, elbows, diffusers, e.t.c.) for the new ventilation duct system developed.

Acknowledgement: The author would like to kindly thank the company Nucair Technologies Sp. z o.o., Solec Kujawski, Poland for the performance of tested ducts and delivery of the air supply system. Authors also received institutional support BS 28/2018 granted by Faculty of Mechanical Engineering of UTP University.

References

1. K. Peszyński, L. Olszewski, E. Smyk, and D. Perczyński, Analysis of the Velocity Distribution in Different Types of Ventilation System Ducts *EPJ Web of Conferences* **180**, 02081 (2018)
2. K. Peszyński, L. Olszewski, E. Smyk., T. Kasprowicz, Development of New Type Ventilation Ducts System, *Proc. of 23rd Int. Conf. EM 2017*, p. 50 – 53, ISBN 978-80-214-5497-2, ISSN 1805-8248 (2017)
3. K. Peszyński, J. Novosád, E. Smyk, L. Olszewski, and P. Dančová, Modelling of air flow rate in significantly flattened rounded rectangular ventilation ducts. *EPJ Web of Conferences* **180**, 02082 (2018)
4. K. Peszyński, Perczyński D., Smyk E., Kolber P. (2017): Experimental Verification of Velocity Distribution in Different Cross-sectional Ventilation Ducts, *Proc. of 23rd Int. Conf. EM 2017*, p. 770 – 783, ISBN 978-80-214-5497-2, ISSN 1805-8248
5. E. Smyk, P. Mrozik P.,S. Wawrzyniak, K. Peszynski (2017): Tabular Air Deflector in Ventilation Ducts, *Proc. of 23rd Int. Conf. EM 2017*, p. 882 – 885, ISBN 978-80-214-5497-2, ISSN 1805-8248